

## QUANTITATIVE THEORY OF RAINBOWS

V.F. Terzi, F.S. Yakupova and L.V. Kurt

Received November 14, 1988

*The first two elements of the light-scattering matrix for a nondispersed, homogeneous system of water particles with a radius of 0.5 mm and a polydispersed system of spherical particles (Deirmendjian's model C.6 cloud) were calculated exactly using the formulas of Mie's theory. The calculations were performed for violet, dark-blue, light-blue, green, yellow-green, orange, red and purple visible radiation. The spectral distributions of the scattering phase function in the region of the primary (scattering angles of 136-142°) and secondary (124-130°) rainbows are presented.*

The theory of the scattering of light by uniform spherical particles has been studied in detail and it is employed to solve many applied problems of the optics of the atmosphere<sup>1-3</sup>. The computational algorithms employed in so doing (for example, Refs. 2 and 4) become unstable for large particles owing to the accumulation of roundoff errors in the calculation of the amplitude functions ascending recurrence relations<sup>4</sup>.

Stable algorithms are required<sup>7</sup> in order to describe quantitatively optical phenomena, such as, rainbows<sup>5</sup>, glories<sup>6</sup>, aureoles, etc., produced by large particles. At the present time no accurate computational data on the optical characteristics (OC) of large spherical particles have been published. For example, in Ref. 8 only the time required to calculate the elements of the scattering matrix for particles with  $\kappa \leq 5000$  ( $\kappa = 2\pi r/\lambda = kr$ , where  $r$  is the radius of the particle,  $\lambda$  is the wavelength of the radiation, and  $k$  is the wave number) is given.

The theory of rainbows constructed in Refs. 5 and 9 is based on computational data on the OC of particles with  $x \leq 1500$  and for a refractive index  $m = 1.33$ , corresponding to the single wavelength  $\lambda = 0.550 \mu\text{m}$ . In this case the spectral variations of the refractive index of water and of the dimensionless parameter  $x$  are ignored, even though it is precisely this dependence that determines the brilliant color distribution in a rainbow. Table 1 gives the values of the complex refractive index of water  $m = n - i\alpha$  and the parameter  $x$  for particles with radius  $r = 0.5 \text{ mm}$ , which we employed to calculate the spectral brightness of a rainbow for the principal wavelengths of visible radiation. The radius of the particles is assumed to be 0.5 mm, since for smaller particles such bright colors cannot be observed in both rainbows.

### COMPUTATIONAL PROCEDURE

To calculate the complex amplitudes we employed both ascending<sup>4</sup> and descending recurrence relations<sup>7,12</sup>; the latter relations give a stable solution for any particle size. The number  $N$  of terms summed<sup>4,7</sup> depends on the parameter  $x$ . We determined the form

of this dependence based on numerous calculations:

$$N = x + 5x^{1/3} + 2, \quad N = mx + 300, \quad \text{Real}(m) > 1. \quad (1)$$

The first expression is employed for  $x < 300$ , when the calculations are performed using the algorithm of Ref. 2 while the second expression is employed for  $x > 300$  using the algorithm of Ref. 7. To avoid overflow and loss of accuracy a piecewise-discontinuous representation of the Ricatti-Bessel functions is employed (the order of magnitude is dropped)<sup>4</sup>. The calculations were performed on an ES-1033 computer; the computing time for  $x = 5000$  and 182 scattering angles is 35 min.

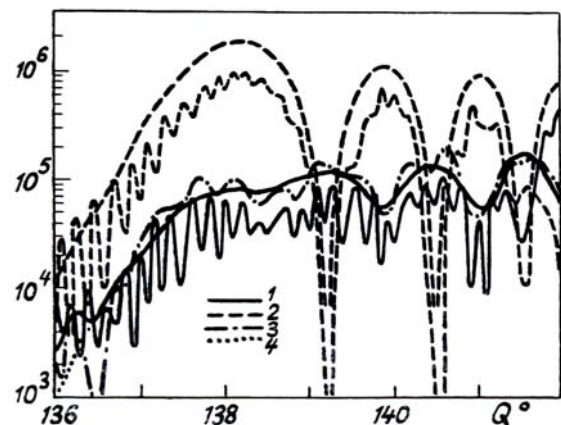


FIG. 1. The two first elements of the scattering matrix in the region of the primary rainbow: parallel (1, 3) and perpendicular (2) components (for  $x = 1500$ ,  $m = 1.33$ ). The smooth curves 1 and 2 were obtained by an approximate method based on Huygens principle<sup>9</sup>; the oscillating curves 1 and 2 our data, calculated exact formulas from Mie's theory; curves 3 and 4 are the data of Ref. 5, obtained based on the exact formulas of Mie's theory (3) and by an approximate method from the theory of complex angular moments.

**RESULTS**

The results for the first two matrix elements in the region of the primary rainbow for  $x = 1500$  and  $m = 1.33$  are compared in Fig. 1. The approximate method based on Huygens principle obviously describes well the behavior of both matrix elements. This method, presented in Ref. 9, is unfortunately applicable only in the region of the primary rainbow and does not describe the finer interference effects responsible for the appearance of the color (usually pink and green) bands (additional arcs) on the inner side of the primary rainbow. The data for the exact calculation (curve 3 in Fig. 1) presented in Ref. 5 refer to the component that does not make a significant contribution to the brightness of the rainbow. As a visual aid our data are shifted downwards by the amount of the attenuation factor  $Q$ , equal to 2.06. In spite of the lack of accurate data on the spectral brightness of a rainbow the angular distribution of the colors in a rainbow was determined more than 100 years ago based on geometric optics.

Geometric optics explains the appearance of rainbows by the existence of extremal angles at which rays emerge from a spherical particle after  $p$  internal reflections<sup>10</sup>. In particular,  $p = 2$  for the primary rainbow and  $p = 3$  for the secondary rainbow.

The scattering angle for these rays can be found based on simple geometric considerations<sup>10</sup>

$$Q_{p-1} = q(2\tau - 2p\tau') + 2\pi c, \tag{2}$$

where the angle of "entry"  $\tau$  of a ray into the particle ( $\tau$ ) and the angle of refraction  $\tau'$  assume extremal values when

$$\tau = \arcsin \sqrt{\frac{m^2 - 1}{p^2 - 1}}, \quad \tau' = \arccos \left[ \frac{1}{m} \cos \tau \right]. \tag{3}$$

For the primary rainbow  $p = 2, c = 0$  and  $q = -1$ ; for the secondary rainbow  $p = 3, c = 1$  and  $q = -1$ . We note that the sign of  $q$  given in Ref. 10 is incorrect in both cases.

As is obvious from (2) and (3) the position of  $Q_{p-1}$  depends on the refractive index  $m$  and the parameter  $p$ . This is the way angular separation of different colors occurs (see Table 1). In addition the color sequence in the primary rainbow  $Q_1$  is reversed with respect to that in the secondary rainbow  $Q_2$ . This phenomenon can also be explained on the basis of geometric optics<sup>10</sup>.

Figures 2 shows the exact calculations of the scattering phase function  $((M_2 + M_1)/2)$  in the region of the primary (a) and secondary (b) rainbows. All the fine effects observable in nature<sup>3</sup> can be seen in these figures. A dark Aleksandrov band can be seen between the rainbows, and narrow bands (especially green and purple-pink) can be seen on the inner side of the primary rainbow and the outer side of the secondary rainbow. As one can see from these figures,  $Q'_1$  and  $Q'_2$  which make the maximum contribution to the scattering phase function, are shifted somewhat for each wavelength  $\lambda$  with respect to the angles  $Q_1$  and  $Q_2$ ; this is attributable to the fact that the angles  $Q_1$  and  $Q_2$  correspond to the extremal values of the angles for  $p = 2$  and  $p = 3$  (see Table 1).

TABLE 1.

*Characteristics of water drop and the main parameters of the primary and secondary rainbows for  $r = 0.5$  mm*

COLOR	CHARACTERISTICS OF A WATER DROP AND THE MAIN PARAMETERS OF THE PRIMARY AND SECONDARY RAINBOWS FOR $r=0.5$ mm										
	$\lambda, \mu\text{m}$	$n$	$\kappa$	$x$	$Q_1$	$P_1$	$Q_2$	$P_2$	$Q'_1$	$Q'_2$	$\theta$
VIOLET	0.375	1.341	$3.5 \times 10^{-9}$	8377.6	139.1	0.903	127.1	0.444	139.4	127.6	2.0035
DARK BLUE	0.400	1.339	$1.86 \times 10^{-9}$	7854.0	138.8	0.985	127.5	0.977	139.1	127.4	2.0042
LIGHT BLUE	0.450	1.337	$1.02 \times 10^{-9}$	6981.3	138.6	0.860	128.1	0.923	138.8	127.6	2.0053
GREEN	0.500	1.335	$1.00 \times 10^{-9}$	6283.2	138.3	0.928	128.5	0.566	138.5	128.2	2.0062
YELLOW-GREEN	0.550	1.333	$1.96 \times 10^{-9}$	5712.0	138.2	0.960	129.1	0.935	138.2	128.5	2.0061
ORANGE	0.627	1.332	$1.39 \times 10^{-8}$	5026.5	137.9	0.865	129.3	0.901	138.1	128.8	2.0055
RED	0.700	1.331	$3.35 \times 10^{-8}$	4488.0	137.8	0.900	129.5	0.806	138.0	129.1	2.0078
PURPLE	0.800	1.339	$1.25 \times 10^{-7}$	3927.0	137.6	0.940	0.796	0.796	137.6	129.6	2.0060

*Note: The angles  $Q'_1$  and  $Q'_2$  correspond to the maximum degree of polarization of the scattered light based on the results of exact calculations for the primary and secondary rainbows;  $\theta$  is the attenuation factor.*

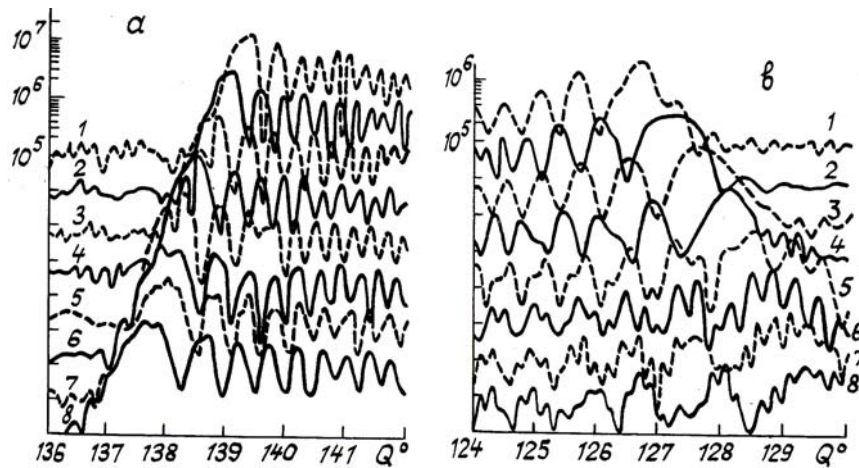


FIG. 2. Scattering phase functions in the region of the primary (a) and secondary (b) rainbow for different wavelengths of visible radiation (the numbers on the curves correspond to the enumeration employed in Table 1). The scale along the ordinate axis pertains to the top curve; the other curves are shifted, as a visual aid, downwards by one unit of the ordinate scale. The discretization step equals 0.1°.

Table 1 also gives the degree of linear polarization of the scattered radiation

$$P = \frac{M_2 - M_1}{M_2 + M_1} \tag{4}$$

for the angles  $Q_1$  and  $Q_2$ , respectively. One can see that the scattered radiation in the region of the rainbow is strongly polarized. The value of  $P$  is significantly higher for  $Q'_1$  and  $Q'_2$ .

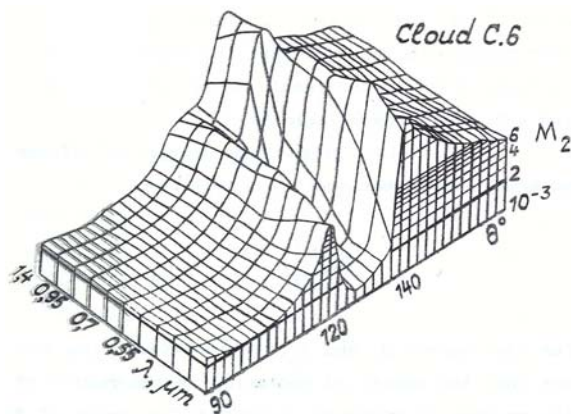


FIG. 3. Diagram of the spectral distribution of the scattering phase function in the region of the primary and secondary rainbows for a polydispersed system of spherical particles (model C. 6 cloud).

The maxima and minima of the scattering phase function beyond the primary peak of the rainbows are associated with the interference of rays undergoing the same number of internal reflections but entering the particle at different angles<sup>10</sup>, so that their position depends strongly on the size of the particle. For a polydispersed system of particles these extrema

are superposed and vanish (Fig. 3). The scattering phase functions presented in Fig. 3 for different wavelengths were calculated for a cloud model in which the particle size distribution is described by a  $\gamma$ -function (model C. 6 cloud)

$$n(r) = 5 \times 10^{-3} r^2 \exp(-0.1r). \tag{5}$$

The data in Fig. 3 refer to the matrix element  $M_2$ , which is the dominant element in the region of the rainbow (see Fig. 1).

Geometric optics describes well the distribution of the spectral brightness of rainbows shown in Figs. 1–3, but a quantitative description is possible only on the basis of Mie's theory. The latter theory actually leads to the multiplication of tens of thousands of complex functions, and this makes it difficult to give a physical explanation of the data so obtained.

Rainbows and glories are characteristic phenomena associated with the scattering of light into the back hemisphere by cloud particles<sup>6</sup>. In both cases the intensity of the scattered light is maximum, but they can be distinguished according to the sign of the polarization: in the rainbow region the electric vector of the scattered radiation is oriented primarily perpendicularly to the scattering plane (positive polarization, i.e.,  $M_2 > M_1$ ); in the glory region (near  $Q = 180^\circ$ ) the electric vector is predominantly parallel to the scattering plane (negative polarization, i.e.,  $M_2 < M_1$ )<sup>6</sup>. Thus the nature of the appearance of nonzero values of the cross-polarized component in the echo signal obtained in the echo signal obtained in polarization laser sounding of clouds<sup>11</sup> can be determined after the sign of the degree of polarization (4) has been determined experimentally: positive polarization should predominate in the case of multiple scattering ( $M_1 > M_2$ ) and negative polarization should predominate in the case of single scattering ( $M_1 > M_2$ ).

## REFERENCES

1. V.E. Zuev, *Propagation of Visible and Infrared Radiation in the Atmosphere* (Sovetskoye radio, Moscow, 1970).
2. V.E. Zuev and G.M. Krekov, *Optical Models of the Atmosphere* (Gidrometeoizdat, Leningrad, 1986).
3. V.E. Zuev and G.M. Kabanov, *Optics of Atmospheric Aerosol* (Gidrometeoizdat, Leningrad, 1987).
4. D. Deirmendjian, *Electromagnetic Scattering on Spherical Polydispersions*, (Elsevier, New York, 1969).
5. Kh. Nussentsveig, *Usp. Fiz. Nauk*, **125**, No. 3, 527 (1978).
6. V.P. Terzi, F.S. Yakupova, A.G. Konyukhov, et al., *Optika Atmosfery*, **1**, No. 8, 51 (1988).
7. G.W. Kattawar and G.N. Plass, *Appl. Opt.*, **6**, No. 8, 1377 (1967).
8. W.I. Wiscombe, *Appl. Opt.*, **19**, No. 9, 1505 (1980).
9. S.D. Mobbs, *J. Opt. Soc. Am.*, **69**, No. 8, 1989 (1979).
10. H. Van de Hulst, *Light Scattering by Small Particles*, (Wiley, New York, 1957).
11. G.M. Krekov, S.I. Kavkyanov and M.M. Krekova, *Interpretation of Signals of Optical Atmospheric Sounding Signals*, (Nauka, Novosibirsk, 1987).
12. K.S. Shifrin and I.L. Zelmanovitch, *Tables of Light Scattering* (Gidrometeoizdat, Leningrad, 1968).